

We are IntechOpen, the world's leading publisher of Open Access books Built by scientists, for scientists

4,800

Open access books available

122,000

International authors and editors

135M

Downloads

Our authors are among the

154

Countries delivered to

TOP 1%

most cited scientists

12.2%

Contributors from top 500 universities



WEB OF SCIENCE™

Selection of our books indexed in the Book Citation Index
in Web of Science™ Core Collection (BKCI)

Interested in publishing with us?
Contact book.department@intechopen.com

Numbers displayed above are based on latest data collected.
For more information visit www.intechopen.com



Polarization Properties of the Solitons Generated in the Process of Pulse Breakup in Twisted Fiber Pumped by ns Pulses

Ariel Flores Rosas, Orlando Díaz Hernández, Roberto Arceo, Gerardo J. Escalera Santos, Sergio Mendoza Vázquez, Elizeth Ramírez Álvarez, Christian I. Enriquez Flores and Evgeny Kuzin

Abstract

Common optical fibers are randomly birefringent, and solitons formatting and traveling in them are randomly polarized. However, it is desirable to have solitons with a well-defined polarization. With pump relatively long pulses, the nonlinear effects of modulation instability (MI) and stimulated Raman scattering (SRS) are dominant at the initial stage of the process of supercontinuum (SC) generation; modulation instability results in pulse breakup and formation of short pulses that evolve finally to a bunch of solitons and dispersive waves. We do the research of the polarization of solitons formed by the pulse breakup process by the effect of modulation instability with pump pulses of nanoseconds in standard fiber (SMF-28) with circular birefringence introduced by fiber twist, and the twisted fiber mitigates the random linear birefringence. In this work, we found that polarization ellipticity of solitons is distributed randomly; nevertheless, the average polarization ellipticity is closer to the circular than the polarization ellipticity of the input pulse. In the experimental setup, 200 m of SMF-28 fiber twisted by 6 turns/m was used. We used 1 ns pulse to pump the fiber. The results showed that at circular polarization of the input pulse solitons at the fiber output have polarizations close to the circular, while in the fiber without twist, the soliton polarization was random.

Keywords: fiber optic, nonlinear optics, pulse propagation and temporal solitons, birefringence and polarization, stimulated Raman scattering

1. Introduction

One of the important mechanisms for the generation of supercontinuum (SC) is the formation of solitons by the nonlinear effect of modulation instability. One feature of the common optical fibers is that they are randomly birefringent, and therefore the generation of solitons and the transition of them by these fibers generated by the nonlinear effects are randomly polarized. Solitons with a well-defined

polarization are necessary for some applications like supercontinuum generation. The propagation of a pulse in a low birefringence fiber using coupled nonlinear Schrödinger equations was considered in [1–3]. In these works, the investigation concludes that the fractional pulses in each of the two polarizations trap each other and move together as one unit which is called a vector soliton. The frequency of each pulse is shifted to compensate the difference in group velocities caused by birefringence. It has been reported the experimental observation of vector solitons [4]. The vector solitons have attracted more attention in applications with linearly birefringent fibers. For the case of fibers with circular birefringence, a special case is when circular birefringence is induced when the fibers are twisted. These twisted fibers can present special advantages for some laser applications. The especial characteristic of twisted fiber is that it induces circular birefringence and eliminates the random linear birefringence [5]. An important consequence of this result is that twisted fiber is less sensitive to environmental conditions and with this we can find new useful features for nonlinear applications [6]. This helps us make the twisted fiber less sensitive to environmental conditions and provides new useful features for nonlinear applications [6]. In [7], it has been analyzed the polarization behavior of vector solitons in a circularly birefringent fiber. In this work, for analysis, we used the two coupled propagation equations in a circularly birefringent fiber that include self-phase modulation, cross phase modulation, and the soliton self-frequency shift [8]. We consider the polarization dependence of the Raman amplification unlike the previously published works [9]. We work on the equations to make a transformation to reduce them to a form of perturbed Manakov task. For our case, the equations were considered as a perturbation unlike the Manakov integrable case. For the case of the perturbation method, we can get the equations for the analysis of the development of evolution of the polarization state of pulses. An important result when analyzing the equations shows that for circularly birefringent fiber (twisted fiber), the cross-polarization Raman term leads to unidirectional energy transfer from the slow circularly polarized component to the fast one. The product of the birefringence and the amplitudes of both polarization components determine the importance of this effect. From all of the above, we can conclude that solitons with any initial polarization state will eventually develop circularly stable polarized solitons.

The split-step Fourier method was used for the numerical analysis of the two coupled nonlinear Schrödinger equations. The parameters of a standard fiber (SMF-28) were used with delay between left- and right-circular polarizations of 1 ps/km that corresponds to circular birefringence in a twisted fiber by 6 turns/m. Furthermore, by the numerical analysis, it is possible to analyze the polarization of solitons generated by the modulation instability effect. An input pulse of 30 ps with 40 W of power was used with a noise imposed which was launched to the fiber input. The input pulses had different polarization ellipticity from circular to linear. From the results, it was found that polarization ellipticity of solitons does not coincide with the polarization of the input pulses. An important result that was also found is that polarization ellipticity of solitons is distributed randomly, but the average polarization ellipticity is mostly circular compared to polarization ellipticity of the input pulse. In the experimental and numerical analysis, SMF-28 standard fiber twisted with 60 y 200 m of length with a pump pulse of 1–10 ns in a wavelength of about 1550 nm was used. The output signal at the fiber end is separated in circular-right and circular-left polarization. The ellipticity of the pulses is calculated with the ratio between the output pulses. The experimental results show that circularly polarized pulses in a fiber with circular birefringence (twisted fiber) are promising for the generation of supercontinuum with stable polarization and confirm the principal conclusions of the modeling propose in [8]; the polarization properties of supercontinuum are also an important issue for application [9–13].

2. Equations to analyze

The equations that describe self-frequency shift of picosecond pulses with linear polarization can be written as follows [14]:

$$\partial_z A_x = i\gamma \left[T_R \partial_T |A_x|^2 \right] A_x \quad (1)$$

the terms A_x , γ , and T_R in Eq. (1) are the envelope of the pulse with linear polarization on the x-axis, the nonlinearity, and the Raman response time, respectively. If the pulse has elliptical polarization, two polarization components have to be included if the input pulse has elliptical polarization, for this case the nonlinear effect of self-frequency shift is considered as dependent on the sum of the powers of the orthogonal components [9]. From the above, it can be said that the value of the parallel Raman gain is equal to the orthogonal Raman gain; the parallel Raman gain is when the pump and Stokes have the same linear polarization, and the orthogonal Raman gain is when the pump and Stokes are polarized orthogonally. The experimental results show that the Raman gain caused by the perpendicular component has a value of 0.3 of the Raman gain for parallel component for a small Stokes shift [15]. For this reason, we used the following equations for the self-frequency shift effect:

$$\partial_z A_x = i\gamma \left[T_R \partial_T |A_x|^2 \right] A_x + i\alpha\gamma \left[T_R \partial_T |A_y|^2 \right] A_x \quad (2)$$

$$\partial_z A_x = i\gamma \left[T_R \partial_T |A_x|^2 \right] A_x + i\alpha\gamma \left[T_R \partial_T |A_y|^2 \right] A_x \quad (3)$$

here $\alpha = \alpha_{\perp}/\alpha_{\parallel}$, where α_{\perp} and α_{\parallel} denote, respectively, the perpendicular and parallel Raman gains.

Using circularly polarized components, we can obtain the equation for the right- and left-circularly polarized state as follows:

$$\partial_z A_+ = \frac{i\gamma T_R}{2} \left\{ \frac{1+\alpha}{2} \partial_t (|A_+|^2 + |A_-|^2) A_+ + (1-\alpha) \partial_t [\text{Re}(A_+ A_-^*)] A_- \right\} \quad (4)$$

$$\partial_z A_- = \frac{i\gamma T_R}{2} \left\{ \frac{1+\alpha}{2} \partial_t (|A_+|^2 + |A_-|^2) A_- + (1-\alpha) \partial_t [\text{Re}(A_+ A_-^*)] A_+ \right\} \quad (5)$$

Eqs. (4) and (5) are the coupling equations describing the self-frequency shift. Adding group velocity dispersion (GVD) and walk-off between circularly polarized components, self-phase modulation (SPM), and cross-phase modulation (XPM) terms to these equations, we have coupling equations that we analyzed analytically and numerically:

$$\begin{aligned} \partial_z A_+ + \beta_1 \partial_t A_+ + \frac{i\beta_2}{2} \partial_t A_+ &= \frac{2i\gamma}{3} (|A_+|^2 + 2|A_-|^2) A_+ \\ &- \frac{i\gamma T_R}{2} \left\{ \frac{1+\alpha}{2} \partial_t (|A_+|^2 + |A_-|^2) A_+ + (1-\alpha) \partial_t [\text{Re}(A_+ A_-^*)] A_- \right\} \end{aligned} \quad (6)$$

$$\begin{aligned} \partial_z A_- - \beta_1 \partial_t A_- + \frac{i\beta_2}{2} \partial_t A_- &= \frac{2i\gamma}{3} (|A_-|^2 + 2|A_+|^2) A_- \\ &- \frac{i\gamma T_R}{2} \left\{ \frac{1+\alpha}{2} \partial_t (|A_+|^2 + |A_-|^2) A_- + (1-\alpha) \partial_t [\text{Re}(A_+ A_-^*)] A_+ \right\} \end{aligned} \quad (7)$$

To describe the above equations, the last two terms on the left side are the effects of Walk-off and Group Velocity Dispersion (GVD) respectively, the terms

in parenthesis of right side are the effects of Self Phase Modulation (SPM) and Cross Phase Modulation (XPM), and finally the terms in key of right side are the Stimulated Raman Scattering effect.

The vector soliton can be approximated by the next equations (not taking into account phases),

$$|A_+(z)| = A \cos(\theta) \operatorname{sech} \left[A(t - t_0) / \sqrt{|\beta_2|} \right], \quad (8)$$

$$|A_-(z)| = A \cos(\theta) \operatorname{sech} \left[A(t - t_0) / \sqrt{|\beta_2|} \right]. \quad (9)$$

And finally applying the perturbation method [16] to Eqs. (6) and (7), we can define the ratio between powers of circularly left- and right-polarized components as follows [7]:

$$\frac{|A_-(z)|}{|A_+(z)|} = \tan(\theta(0)) \exp \left[\frac{2(1 - \alpha)}{3} \gamma A^2 \frac{T_R \beta_1}{|\beta_2|} z \right]. \quad (10)$$

From Eq. (10), we can see that the change of the polarization ellipticity of the vector soliton along the fiber may occur only in the presence of circular birefringence (twisted fiber, β_1 is not equal to 0).

3. Numerical results

The split-step Fourier method is used for solving Eqs. (6) and (7) [14]. The values of using parameters are the following: $\beta_1 = 1$, $\beta_1 = -1$ ps/km; $\beta_1 = 0$; $\beta_2 = -25$ ps²/km, $\alpha = 0.3$, $\gamma = 1.6$ 1/(W-km), $T_R = 3$ fs. The value of $\beta_1 = 1$ corresponds to the twisted fiber with 6 turns/m. The meaning of the change of the sign of the constant β is for representing the change of the twist direction. For simulations, the 30 ps input pulse with 40 W power in the input fiber was used, and the Gaussian noise was added on the pulse. Modulation instability (MI) effect breaks up the pulse generating a set of solitons; the highest soliton were traced in this set [8].

When a linearly polarized pulse is introduced to the fiber input, we can see the influence of the walk-off effect between circularly right- and left-polarized components on ellipticity, see **Figure 1**. The fiber optic length used varies from 1 to 1.5 km. The results for the simulations are present in **Figure 1**, the result for $\beta_1 = 1$ is shown by open circles, for $\beta_1 = -1$ is shown by closed circles, and for $\beta_1 = 0$ is shown by squared. The important result for the dependence of polarization behavior can be observed clearly. The polarization behavior with $\beta_1 = 1$, but in this special case, we consider $\alpha = 1$, that is, the parallel Raman gain is equal to the perpendicular, $\alpha = 1$, see **Figure 2**. It can be seen that in this case, the effect of the ellipticity change of the soliton along the fiber is not presented. The results obtained are based on Eq. (10), and these results show that some ellipticity change must be presented on the circular birefringence and difference between Raman parallel and perpendicular gain. It can be observed that the ellipticity of the highest soliton does not coincide with the ellipticity of the input pulse (there is an exception for the case where $\beta_1 = 0$).

For the special case when using elliptical input polarization, the results show a similar behavior of the polarization ellipticity to make the energy transform from the slow to fast circularly polarized component. With these results, it can be said that the soliton with a fast circular polarization component propagates in the fiber with stable polarization. From the case of Eq. (10), we can say that this equation describes the polarization evolution of the soliton, but it is not applicable for

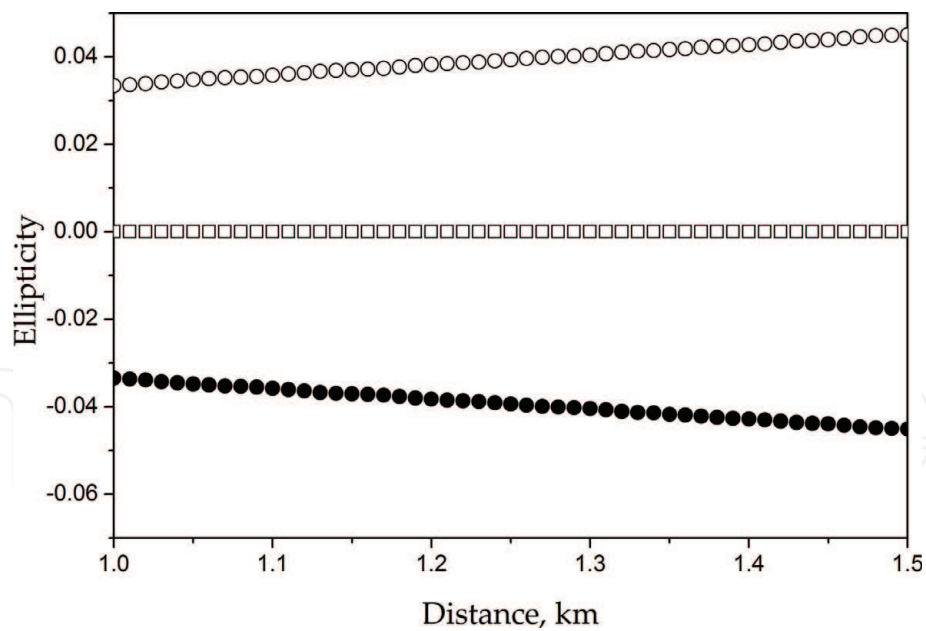


Figure 1. Ellipticity vs. fiber length for a soliton with linearly polarized pulse at the entrance for $\beta_1 = 1$ (closed circles), $\beta_1 = -1$ (open circles), and $\beta_1 = 0$ (squared).

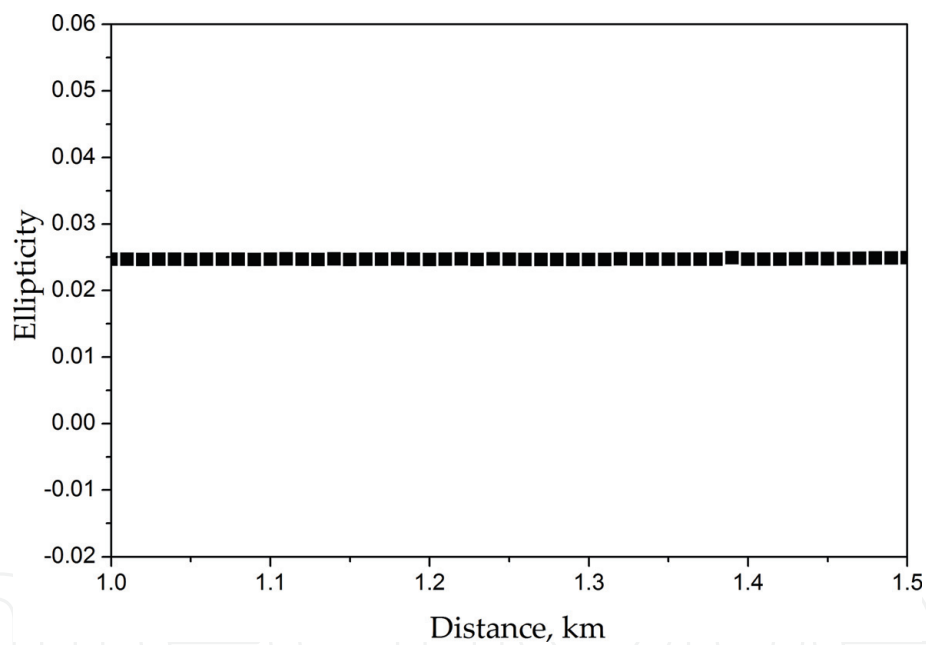


Figure 2. Ellipticity vs. fiber length for linear input pulse, particularly for the case when parallel Raman gain is equal to perpendicular Raman gain.

development of the process of the soliton formation. As we can see from the previous results, the polarization of the soliton at the end of the soliton formation process does not coincide with the polarization of the input pulse. The process of generation of solitons by the effect of modulation instability is complex, and the stochastic process depends on the noise. It was calculated by the ellipticity of solitons generated in the process of the effect of modulation instability for different noise imposed on the input pulse. The ellipticity of the highest solitons was found to be randomly distributed. In **Figure 3**, the number of solitons that were generated with different ellipticity when linearly polarized input pulse was used is showed; the total of number of calculation was 150. As you can see, the polarizations of solitons are mostly concentrated close to the linear one; however, solitons with a wide range of the polarization ellipticity can also appear. **Figure 3** shows that the

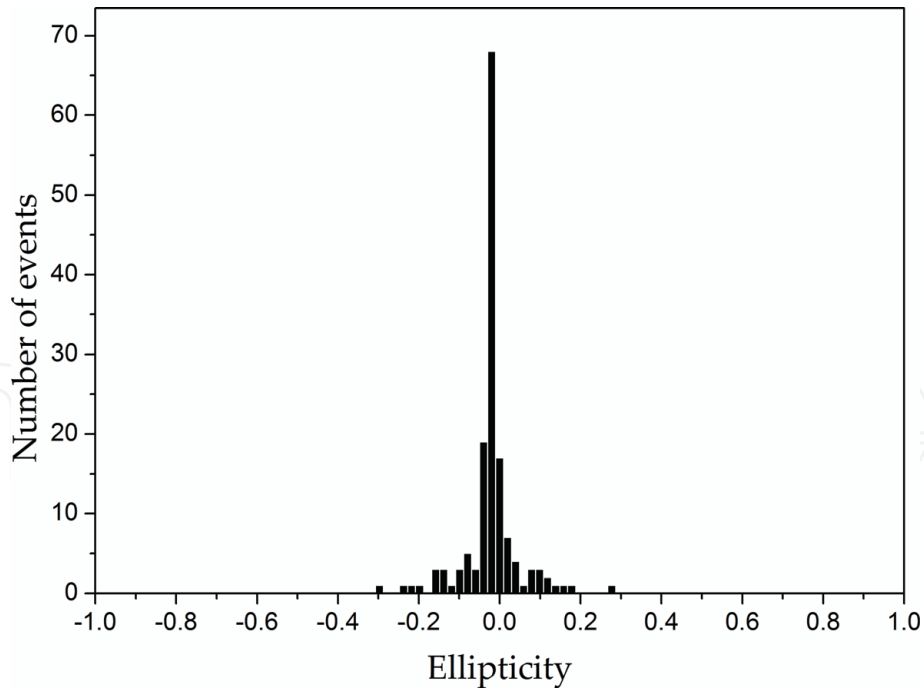


Figure 3.
The number of solitons with different ellipticity generated by the effect of modulation instability at linear polarization of the input pulse.

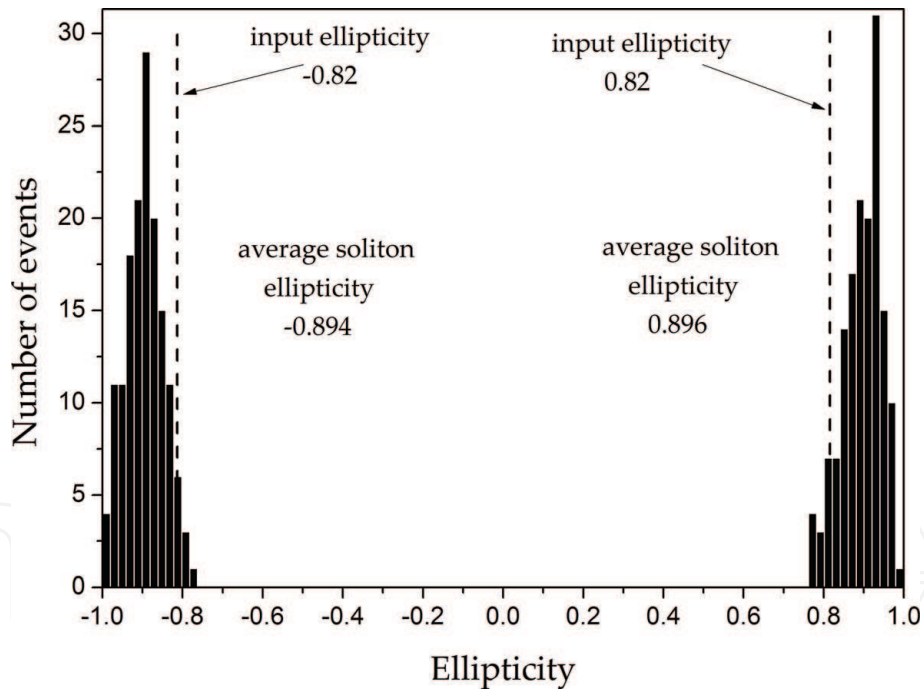


Figure 4.
The number of solitons with different ellipticity generated by modulation instability at polarization of the input pulse of 0.82 and -0.82 .

average polarization ellipticity of solitons is -0.02 . The maximum ellipticity found in this set of calculations was 0.3.

The distribution of polarization of solitons when the input pulse has ellipticity of 0.82 is showed in **Figure 4**. From **Figure 4**, it can be observed that the average soliton polarization moves toward circular polarization. For the case when the polarization of the input pulse is close to the circular polarization, the dispersion of the polarization ellipticity of solitons becomes much less, see **Figure 5**. For **Figure 5**, the polarization ellipticity of the input pulse used was equal to 0.906 and -0.906 . It

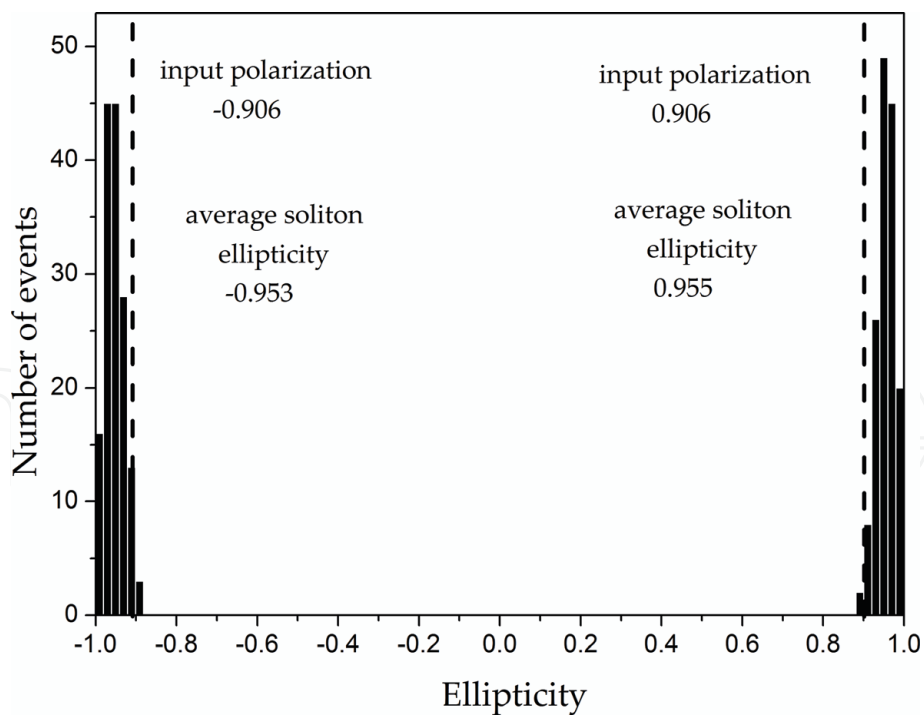


Figure 5.
 The number of solitons with different ellipticity generated by modulation instability at polarization of the input pulse of 0.906 and -0.906 .

can be seen that most of the solitons have the ellipticity closer to the circular polarization than the input pulse. Average ellipticity of solitons in this case was found to be about 0.95.

4. Experimental setup

In **Figure 6**, the experimental setup is showed. For the source of signal, a continuous wave distributed feedback semiconductor laser with a wavelength of 1550 nm was used. The continuous wave signal was gated and amplified by the erbium doped fiber amplifier (EDFA) from which you can get pulses with 1–10 ns duration and a maximum peak power of about 150 W. To assure the stable polarization state, the pulses from the EDFA pass through a polarization controller (PC) and a polarizer. With the rotation of quarter wave retarder (QWR1), we can change the polarization ellipticity to be able to control the input polarization on the fiber. The output of the fiber under the test (twisted fiber) is connected to a quarter wave retarder (QWR2) and polarization beam splitter (PBS). The QWR2 and PSB convert the right and left circularly polarized component at the output fiber to orthogonally polarized linear components at the output PBS. The output of PSB (linearly polarized component) is separated in time by a delay line (10 m of SMF-28 fiber), and they come together using a 50/50 coupler to launch the same monochromator input. The output pulses are detected and monitored by an oscilloscope. A typical

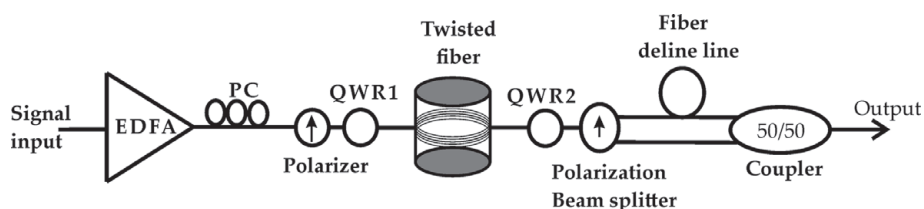


Figure 6.
 Experimental setup.

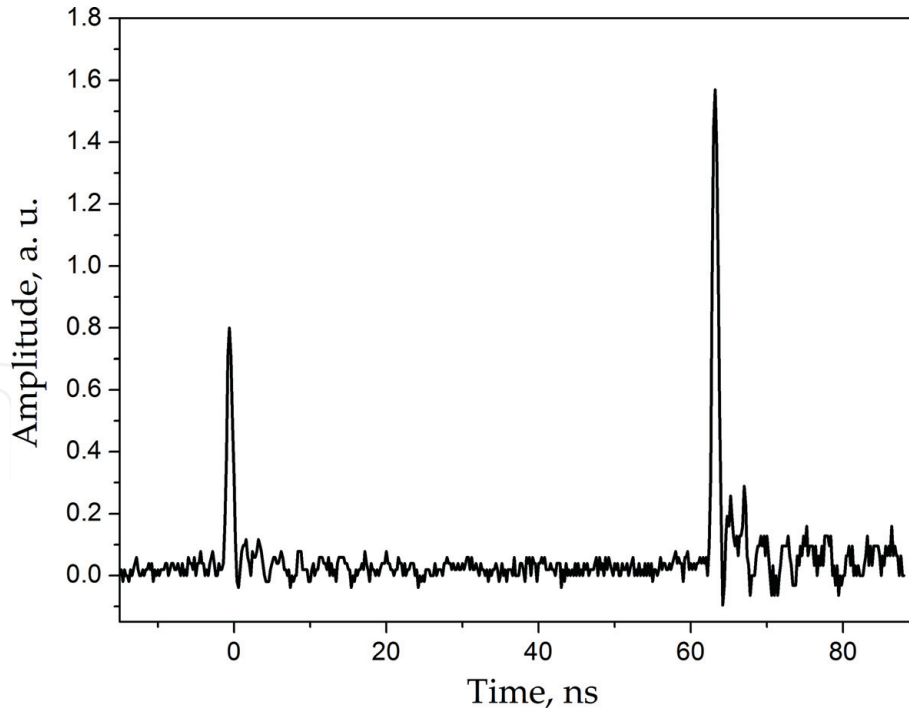


Figure 7.
A typical oscilloscope trace.

oscilloscope trace is shown in **Figure 7**. The first pulse is that traveling from a port 1 of the polarization beam splitter, and second pulse travels from a port 2 of the polarization beam splitter through the delay line (10 m of SMF-28 fiber). With this experimental setup, we can measure the amplitudes of left and right circularly polarized component at any wavelength using one single shot in the oscilloscope [17]. The ellipticity is calculated using the next equation:

$$\rho = \tan^{-1} \left(\frac{\sqrt{P_+} - \sqrt{P_-}}{\sqrt{P_+} + \sqrt{P_-}} \right) \quad (11)$$

where P_+ and P_- are the pulse amplitudes at the monochromator output. A disadvantage of this method is that we measure the average ellipticity of the bundle of solitons.

We used span of SMF-28 fiber with different lengths, twisted, and without twist. To calibrate the ellipticity measurement system, the ellipticity was measured at the polarizer output. The results of measurements are presented in **Figure 8**. The angle 0 on the position of the QWR1 corresponds to linearly polarized signal at the QWR1 output. Taken into account that the ellipticity of the signal at the QWR1 output is equal to the angle of the rotation of QWR1 in the range $-45^\circ + 45^\circ$ [18]. The maximum ellipticity measured was 35° . At this ellipticity, 97% of the power is in one circularly polarized component and only 3% is in orthogonal component. In our setup, the measurement of the higher ellipticity is restricted by the possibility of the measurement of low power pulse. In the experiment, it was used 1-ns pump pulse with a maximum power of 150 W and a wavelength of 1550 nm. Linearly polarized pump pulses passed through QWR1. The angle of QWR1 defined the polarization state of the input pulse that is launched to the fiber. In the experiment, the span of SMF-28 fibers was used with lengths of 65 and 218 m. The fibers under the test were twisted with a twist of 6 turn/m and they were put on the cylinder with diameters of 25 and 50 cm. From the experimental results, it can be observed that both fibers conserved the polarization ellipticity along the fiber at low powers. **Figure 8** shows the ellipticity of the low power continuous wave (CW) radiation at the output of

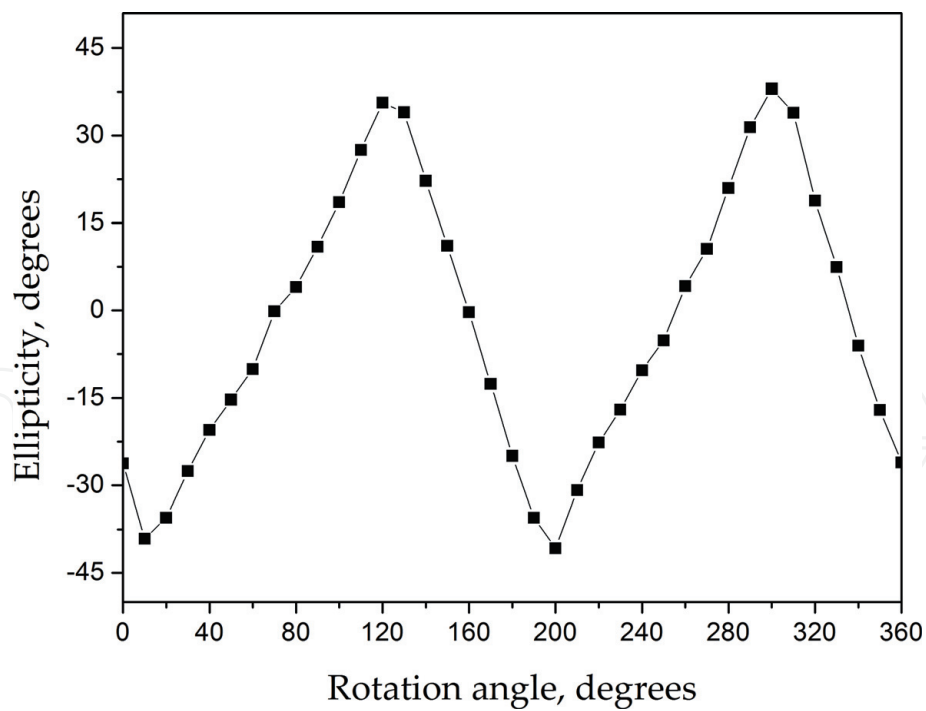


Figure 8.
 Ellipticity at the QWR1 output measured by our setup.

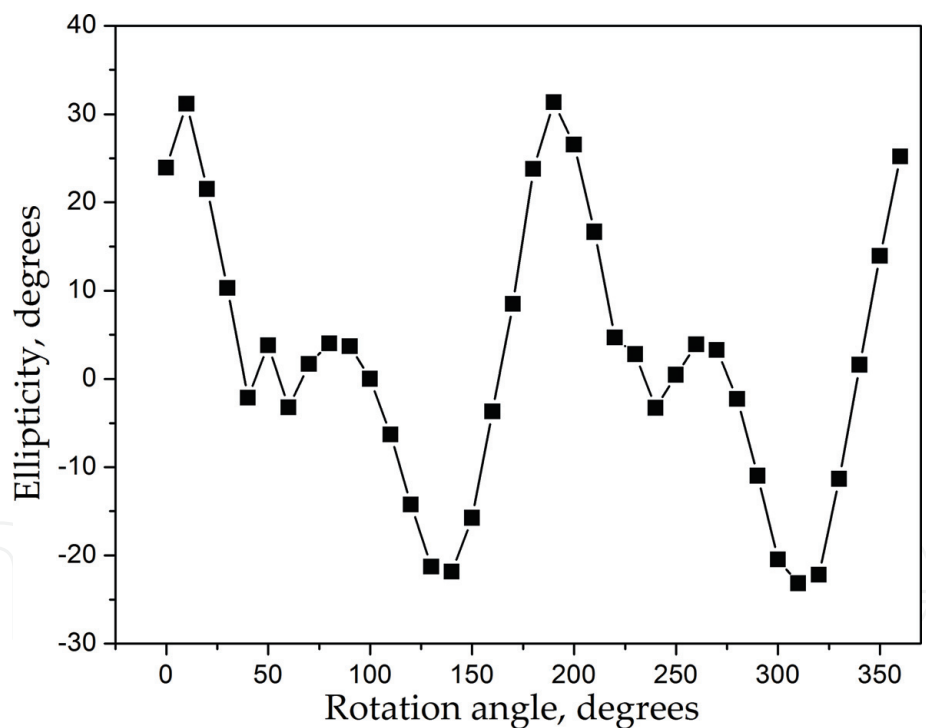


Figure 9.
 The ellipticity at the output of the 218-m fiber without twist.

the 65-m SMF-28 fiber. It can be observed that the dependence is the same as the dependence of the ellipticity on the QWR1 angle at the fiber input.

Next step was the measurements of the ellipticity at the fiber output at low power. These measurements show the effect of residual linear birefringence in the fiber. In **Figure 9**, we show the ellipticity at the output of the 218-m fiber without twist. As another example, **Figure 10** shows the ellipticity at the output of the 218-m twisted fiber wound on the cylinder with a diameter of 25 cm (squares); **Figure 10** shows the ellipticity at the output of the same fiber however wound on the cylinder with a diameter of 50 cm (circles). **Figure 10** (for fiber wound on the

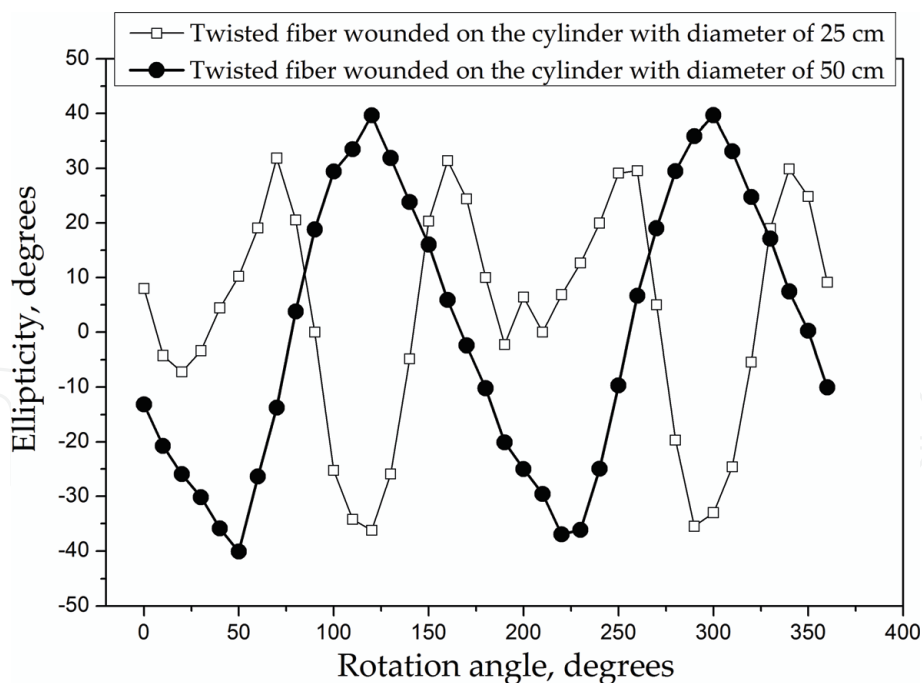


Figure 10.

The ellipticity at the output of the 218-m fiber: squares—on 25-cm cylinder and circles—on the 50-cm cylinder.

cylinder with a diameter of 50 cm) shows the ellipticity at the fiber output is the same as at the fiber input. It means that there is no effect of linear birefringence. However, for the 25-cm diameter cylinder, the effect of the linear birefringence can be clearly seen.

When the pulses with the power of 150 W were launched to the input fiber, the pulse breakup occurred followed by the soliton formation and soliton self-frequency shift; see **Figure 11**. The polarization ellipticity was measured at the output of the 218-m twisted fiber on the 50-cm cylinder and also at the output fiber with the same length but without twist. The measurements were done for high power wavelengths of 1560, 1570, and 1580 nm. The results for these wavelengths are presented in **Figures 12–14**, for 1560, 1570, and 1580 nm, respectively. For these results, it can be seen that solitons at the output of twisted fiber present a high grade of polarization at least when the input polarization has circular polarization, for the angle of QWR1 of about 50° . We can use Eq. (11) to calculate that about 90% of output power is in the same circular polarization as in the output and only about 10% in the orthogonal polarization. With this technique used, we can measure the averaged polarization, and so if measured ellipticity is close to 0, it does not imply that solitons have linear polarization, it just means that powers of all solitons in the selected spectral range in both circularly polarized components are equal. For the case of the fibers without twist, the polarization is chaotic. It can be seen that for the wavelengths of 1570 and 1580 nm, where the measured ellipticity is very close to 0 [17]. There are no physical reasons for the linear polarization at any input polarization; so we can think that the polarization ellipticity of solitons most probably is random.

The slope of the dependencies of the output ellipticity on the input at the input ellipticity equal to 0 is equal to 1.9 for wavelengths 1570 and 1580 nm and 0.9 for 1560 nm. The fact that the slope is higher than in 1570 and 1580 nm can show that the output ellipticity tends to be higher than the input ellipticity. The ellipticity of the highest soliton generated in the process of pulse breakup at different noise imposed on the pulse was also calculated. The equations and the procedure described before were used [7]. The equations are taken into account the difference of group velocity of orthogonal circularly polarized components and vectorial nature of the Raman

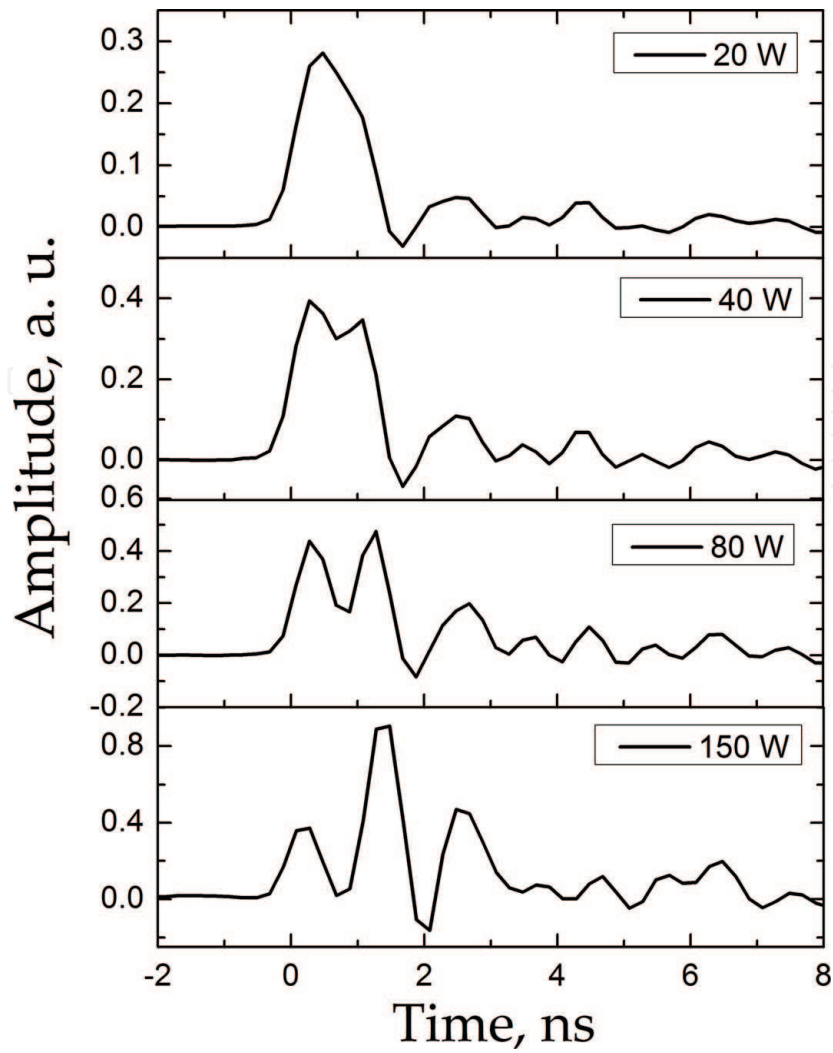


Figure 11.
The process of the pulse breakup.

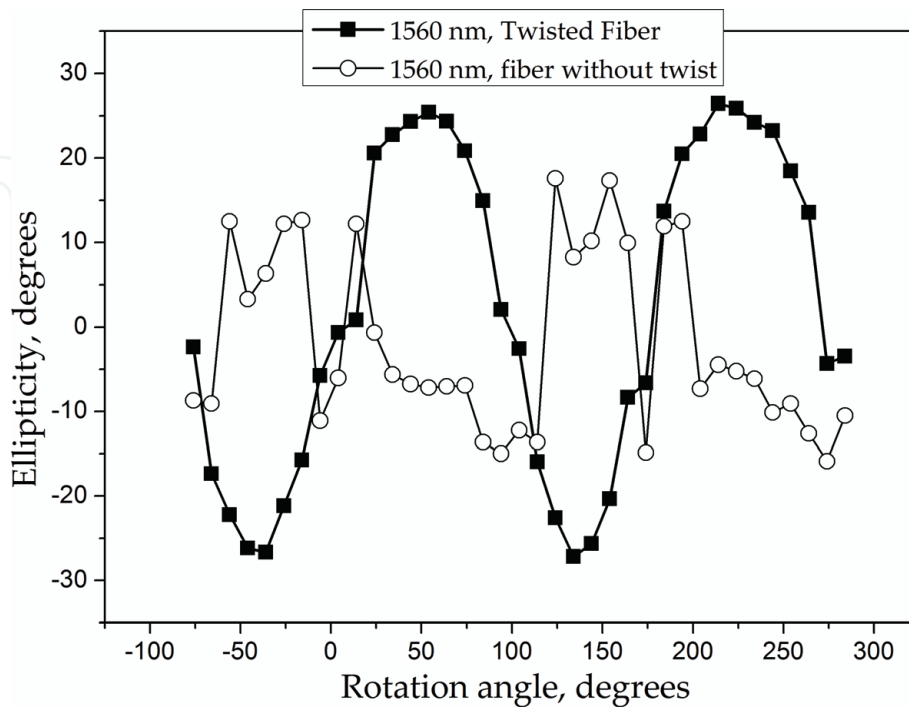


Figure 12.
The ellipticity at the output of the 218-m fiber for 1560 nm: squares for the twisted fiber and circles for the fiber without twist on the 50 cm cylinder.

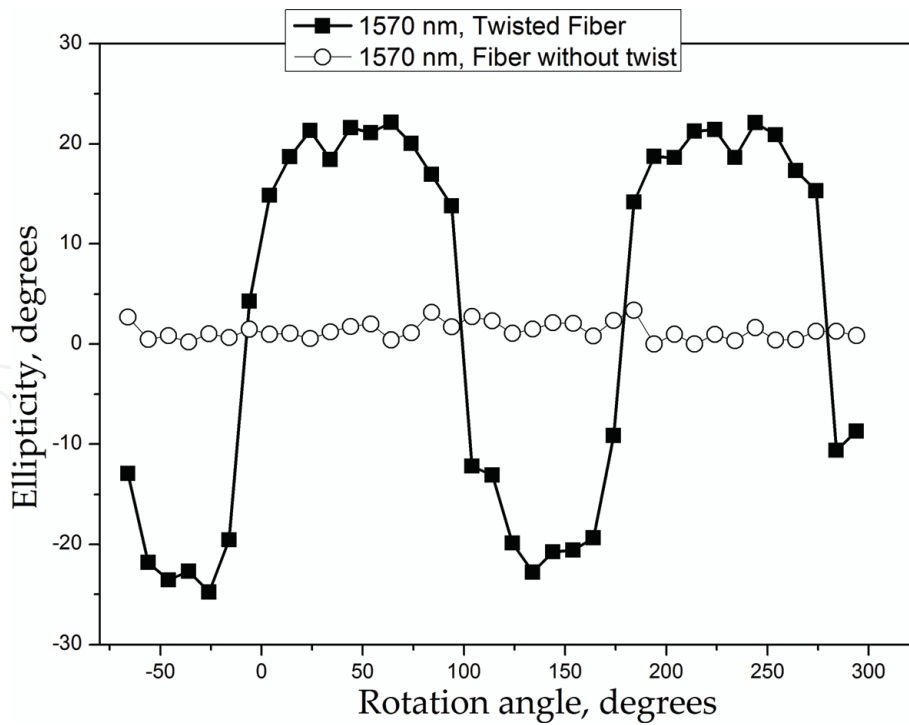


Figure 13. The ellipticity at the output of the 218-m fiber for 1570 nm: squares for the twisted fiber and circles for the fiber without twist on the 50 cm cylinder.

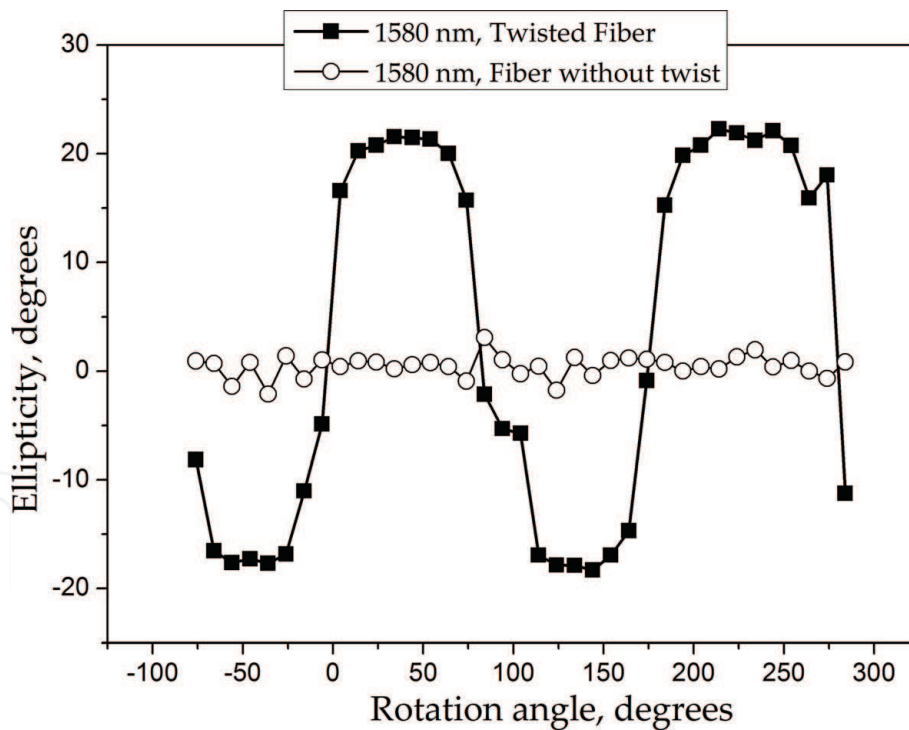


Figure 14. The ellipticity at the output of the 218-m fiber for 1580 nm: squares for the twisted fiber and circles for the fiber without twist on the 50-cm cylinder.

effect in the optical fiber. Like in **Figure 15**, we have examples of the 50 calculations with 30 ps input pulse with 40 W of power. For the numerical calculation, the following parameters were used: $\beta_1 = 0.2$ ps/km and $\beta_2 = 25$ ps²/km. The input polarizations were equal to 0.4 (equal to 21.8°) and 0.9 (equal to 42°). As we can see in most of the realizations, the output ellipticity of the solitons was greater than the ellipticity of the input pulse. For the case when input ellipticity is equal to 0.4, the

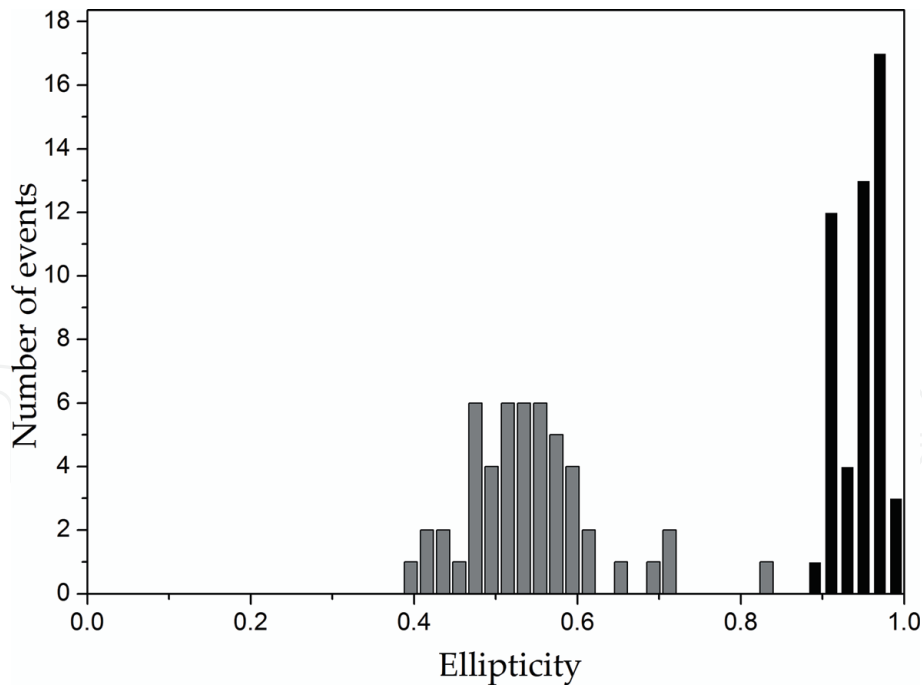


Figure 15.
 Statistics of the ellipticity of the highest soliton.

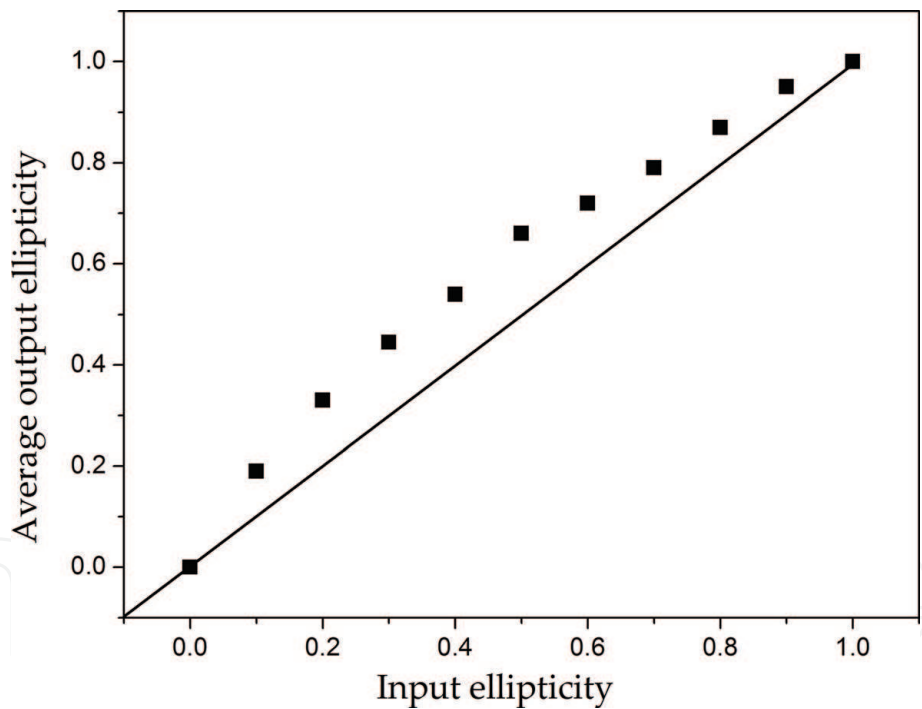


Figure 16.
 Average output polarization vs. input polarization.

average output ellipticity is equal to 0.54, and the case for input ellipticity is equal to 0.9, the average output ellipticity is equal to 0.95, see **Figure 15** [18].

Numerical calculations were done for different input polarizations. The dependence of the average output soliton ellipticity on the input ellipticity is showed in **Figure 16**. The simulations corroborate the measured tendency of soliton to have the higher ellipticity than the input pulse. Simulations show that the fluctuations of the soliton polarization get to be smaller when the input polarization approaches to the circular. We also made calculations for $\beta_1 = 0$, that is, for ideal fiber without any birefringence and found similar statistic for the polarization of solitons.

5. Conclusions

Finally, it can be concluded that the solitons generated in the nonlinear process of pulse breakup for the special case when the twisted standard fiber is used can present a high degree of polarization for the case when the polarization of the input pulse is circular. The numerical calculations agree with the experimental results show that the polarization ellipticity of solitons tends to be greater than the polarization of the input pulse (for the case when the polarization of the input pulse is circular). We can say that according to the results, this effect does not depend on the circular birefringence, so, in this particular case, the twisted fiber plays a role of the ideal fiber without birefringence.

Acknowledgements

The authors thank the Mexican Council for Science and Technology (CONACyT) for providing financial support for the realization of this project and the Publication funded with PFCE 2018 resource (Program for Strengthening Educational Quality).

Author details

Ariel Flores Rosas^{1*}, Orlando Díaz Hernández¹, Roberto Arceo¹, Gerardo J. Escalera Santos¹, Sergio Mendoza Vázquez¹, Elizeth Ramírez Álvarez¹, Christian I. Enriquez Flores² and Evgeny Kuzin³


¹ Faculty of Sciences in Physics and Mathematics, Autonomous University of Chiapas, Tuxtla Gutiérrez, Chiapas, México

² Conacyt Chairs Program, National Council of Science and Technology, México City, México

³ Department of Optics, National Institute of Astrophysics, Optics and Electronics (INAOE), Puebla, México

*Address all correspondence to: ariel.flores@unach.mx

IntechOpen

© 2018 The Author(s). Licensee IntechOpen. This chapter is distributed under the terms of the Creative Commons Attribution License (<http://creativecommons.org/licenses/by/3.0>), which permits unrestricted use, distribution, and reproduction in any medium, provided the original work is properly cited. 

References

- [1] Menyuk CR. Stability of solitons in birefringent optical fibers. I: Equal propagation amplitudes. *Optics Letters*. 1987;**12**(8):614-616
- [2] Menyuk CR. Stability of solitons in birefringent optical fibers. II. Arbitrary amplitudes. *Journal of the Optical Society of America B: Optical Physics*. 1988;**5**(2):392-402
- [3] Christodoulides DN, Joseph RI. Vector solitons in birefringent nonlinear dispersive media. *Optics Letters*. 1988; **13**(1):53-55
- [4] Islam MN, Poole CD, Gordon JP. Soliton trapping in birefringent optical fibers. *Optics Letters*. 1989;**14**(18): 1011-1013
- [5] Tsao C. *Optical Fiber Waveguide Analysis*. New York: Oxford University Press; 1999
- [6] Tanemura T, Kikuchi K. Circular-birefringence fiber for nonlinear optical signal processing. *Journal of Lightwave Technology*. 2006;**24**(11):4108-4119
- [7] Korneev N, Kuzin EA, Villagomez-Bernabe BA, Pottiez O, Ibarra-Escamilla B, González-García A, et al. Raman-induced polarization stabilization of vector solitons in circularly birefringent fibers. *Optics Express*. 2012;**20**(22): 24289
- [8] Kuzin EA, Flores-Rosas A, Peralta-Hernandez JI, Villagomez-Bernabe BA, Ibarra-Escamilla B, Gonzalez-Garcia A, et al. Polarization properties of vector solitons generated by modulation instability in circularly birefringent fibers. In: *Nonlinear Optics and Applications VII*. Vol. 8772. Prague, Czech Republic: SPIE Optics + Optoelectronics. 2013. p. 877218
- [9] Tu H, Liu Y, Liu X, Turchinovich D, Lægsgaard J, Boppart SA. Nonlinear polarization dynamics in a weakly birefringent all-normal dispersion photonic crystal fiber: Toward a practical coherent fiber supercontinuum laser. *Optics Express*. 2012;**20**(2): 1113-1128
- [10] Lehtonen M, Genty G, Ludvigsen H, Kaivola M. Supercontinuum generation in a highly birefringent microstructured fibre. *Applied Physics Letters*. 2003;**82**: 2197-2199
- [11] Xiong C, Wadsworth WJ. Polarized supercontinuum in birefringent photonic crystal fiber pumped at 1064 nm and application to tunable visible/UV generation. *Optics Express*. 2008;**16**: 2438-2445
- [12] Zhu Z, Brown TG. Polarization properties of supercontinuum spectra generated in birefringent photonic crystal fibers. *Journal of the Optical Society of America B: Optical Physics*. 2004;**21**:249-257
- [13] Zhu Z, Brown TG. Experimental studies of polarization properties of supercontinua generated in a birefringent photonic crystal fiber. *Optics Express*. 2004;**12**:791-796
- [14] Agrawal GP. *Nonlinear Fiber Optics*. San Diego, CA, USA: Academic Press; 2001. pp. 48-49
- [15] Mandelbaum I, Bolshtyansky M, Heinz F, Hight R. Method for measuring gain tensor in optical fibers. *Journal of the Optical Society of America B: Optical Physics*. 2006;**23**(4):621-627
- [16] Midrio M, Wabnitz S, Franco P. Perturbation theory for coupled nonlinear Schrödinger equations. *Physical Review E*. 1996;**54**(5):5743-5751
- [17] Flores-Rosas A, Mendoza-Vazquez S, Posada-Ramirez B, Kuzin EA,

Ibarra-Escamilla B. Polarization properties of solitons generated in process of pulse breaking-up in a fiber with circular birefringence. In: Latin America Optics and Photonics Conference, Paper LTu4A47

[18] Flores-Rosas A, Peralta-Hernandez JI, Villagomez-Bernabe BA, Bracamontes- Rodríguez YE, Beltran-Perez G, Pottiez O, et al. Observation of a high grade of polarization of solitons generated in the process of pulse breakup in a twisted fiber. *Journal of the Optical Society of America B: Optical Physics.* **31**:821-826

IntechOpen